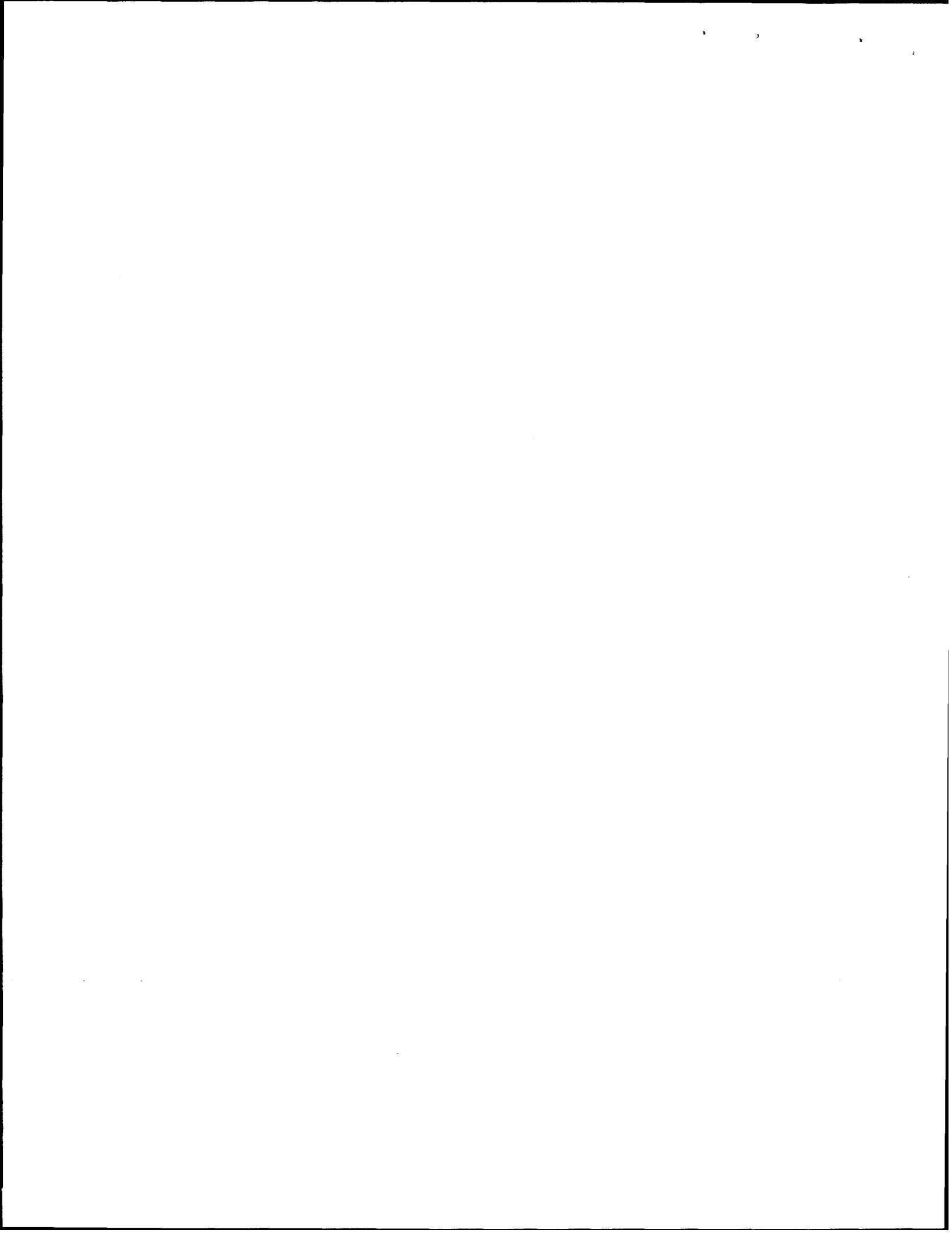


## Work Functions of the Transition Metals and Metal Silicides

Timothy J. Drummond  
Sandia National Laboratories  
Albuquerque, NM 87185-0603

## ABSTRACT

The work functions of polycrystalline metals are often used to systematize Schottky barrier height data for rectifying contacts to semiconductors. Rectifying contacts to silicon devices are predominantly formed using conductive metal silicides with work functions which are not as well characterized as metal work functions. The present work has two objectives. First, it classifies the transition metals using correlations between the metal work function and the atomic chemical potential. Second, the available data for metal silicides is collected and interpreted using an average charge transfer (ACT) model. The ACT model accounts for the electronic hardness of the component elements in addition to their chemical potentials. New trends in the behavior of silicide work functions are identified.



## **DISCLAIMER**

This report was prepared as an account of work sponsored by an agency of the United States Government. Neither the United States Government nor any agency thereof, nor any of their employees, make any warranty, express or implied, or assumes any legal liability or responsibility for the accuracy, completeness, or usefulness of any information, apparatus, product, or process disclosed, or represents that its use would not infringe privately owned rights. Reference herein to any specific commercial product, process, or service by trade name, trademark, manufacturer, or otherwise does not necessarily constitute or imply its endorsement, recommendation, or favoring by the United States Government or any agency thereof. The views and opinions of authors expressed herein do not necessarily state or reflect those of the United States Government or any agency thereof.

## **DISCLAIMER**

**Portions of this document may be illegible in electronic image products. Images are produced from the best available original document.**

## INTRODUCTION

In the 31 years since its publication, the compilation of work functions of polycrystalline elements by Michaelson has been accepted as a standard reference.<sup>1</sup> In a recent analysis of the rare earth and *sp* valent metals it was postulated that the work functions of "good" polycrystalline are truly characteristic of surfaces with a zero net surface dipole.<sup>2</sup> In this case, the work function locates the bulk chemical potential relative to the vacuum reference level. This assumption is frequently and implicitly made when polycrystalline work functions are used to systematize Schottky barrier height data for rectifying contacts to semiconductors. Most rectifying contacts to semiconductors are made with transition metals and the assumption of a zero net surface dipole must be validated for these elements in addition to the rare earth and *sp* valent metals. In the case of contacts to silicon, most technologically important rectifying contacts to silicon are conductive metal silicides. A comprehensive compilation of silicide work functions has not previously been published. It is the goal of this paper to assess the work function values of the transition metals and both transition metal and rare earth silicides for surface contributions.

An assessment of the metallic *sp* valent and rare earth elements has been reported elsewhere.<sup>2</sup> The key result of this previous work was that "good" polycrystalline work functions were characteristic of surfaces with a zero net surface dipole. At metal surfaces negative dipoles arise from the spreading effect as surface electrons "spread" out into the vacuum. Positive dipoles form as electrons flow into low open spaces on atomically rough surfaces.<sup>3</sup> Polycrystalline surfaces allow for both kinds of dipoles and strong correlation between bulk and atomic properties was argued to imply near perfect cancellation to minimize the total surface energy. The polycrystalline

work function may then be taken as a good estimate of the bulk chemical potential of the metal relative to the vacuum level,  $\phi_m = E_{\text{vac}} - \mu$ . The situation is more complex for silicides. One component is an elemental metal with delocalized bonding. The other is a covalent semiconductor with highly directional bonding. It is a finding of the present work that silicon atoms at metallic silicide surfaces appear to inhibit the redistribution of electronic charge into spreading and smoothing dipoles as is characteristic of an elemental metal.

This work catalogs transition metal work functions which are believed to be representative of near zero dipole surfaces. Assumptions are then made to determine the effective number of valence electrons. This allows the hardness of the atoms to be calculated which is, in turn, essential to the calculation of silicide work functions using electronegativity equalization theory.<sup>4</sup> The work functions of transition metal and rare earth silicides are cataloged and compared with theory. Silicides can be classified into three major groups as the metal is a rare earth, early transition metal, or late transition metal. Allowing for a covalency induced surface effects predictions of the silicide work functions are consistent with experimental values.

## THEORY

To evaluate the transition metal elements, trends in the correlation between the metal work function,  $\phi_m$ , and the atomic chemical potential,  $\mu_\alpha$ , derived from the atomic polarizability,  $\alpha$  are studied. This correspondence is studied because a)  $\mu_\alpha$  can be derived experimentally, and b) it is intimately related to the hardness,  $\eta$ , of the valence electrons. Given the electronic charge,  $q$ , of a neutral atom and an energy functional for the atom,  $E(q)$ , the electronegativity is defined as

$$\chi = -\mu = -\delta E(q)/\delta q \quad (1)$$

and the hardness as

$$\eta = (1/2)\delta^2 E/\delta q^2 = (1/2)\delta\chi/\delta q \quad (2)$$

such that the first few terms of a Taylor's series expansion of energy of the atom is<sup>5,6</sup>

$$E(q) = E^0 + \chi q + \eta q^2. \quad (3)$$

In SI units,  $\mu$  and  $\eta$  are expressed in terms of atomic polarizability  $\alpha$  (F m<sup>2</sup>/atom) as

$$\mu_\alpha = e\eta_\alpha = e(4\pi\epsilon_0 n/\alpha)^{1/3}/4\pi\epsilon_0 \quad (4)$$

where  $\epsilon_0$  is the permittivity of free space,  $n$  is the number of valence electrons, and  $e$  is the charge of an electron. A discussion of the correlation of these quantities with various electronegativity scales has been given by Nagle for  $sp$  valent elements.<sup>7</sup>

To evaluate the work functions of metal silicides the concept of electronegativity equalization is applied to the unit formula of the silicide,  $m_x\text{Si}_y$ , where  $m$  substitutes for the metal. In the past, silicide work functions have been estimated as the mean of the metal work function and the work function of Si

$$\phi(m_x\text{Si}_y) = [\phi(m)^x\phi(\text{Si})^y]^{1/(x+y)} \quad (5)$$

with reasonable success.<sup>8</sup> This approach has two flaws. First, it neglects the effect of the hardness on electronegativity equalization. Second, Si is a semiconductor and the accepted Si work function is determined by surface states and is not a bulk property.<sup>9</sup> The appropriate reference level is the intrinsic chemical potential,  $\mu(\text{Si})$  of bulk Si. In studies of metal contacts to semiconductors  $\mu(\text{Si})$  is identified as the charge neutrality level (CNL).<sup>10,11</sup> While this quantity cannot be measured directly theoretical estimates are in good agreement with the inferred position within the semiconductor band

gap.<sup>12</sup> The work function locating  $\mu(\text{Si})$  is 4.66 eV and is 0.19 eV less than the work function locating the surface state band of the Si(111) surface.

In the present paper, the electronegativity equalization formula given by Komorowski<sup>4</sup> is adapted to the estimation of silicide work functions using the metal work function  $\phi_m$  and the silicon work function,  $\phi^* = E_{\text{vac}} - \mu(\text{Si})$ , as

$$\phi(\text{silicide}) = \eta_M [x\phi_m/\eta_\alpha(m) + y\phi^*/\eta_\alpha(\text{Si})] \quad (6)$$

where  $1/\eta_M = x/\eta_\alpha(m) + y/\eta_\alpha(\text{Si})$ .  $\eta_M$  is the average hardness of the unit formula molecule. In Equation 6 the equilibration of the bulk chemical potentials, approximated as  $\phi_m$  and  $\phi^*$ , is moderated by the atomic hardnesses.

## DATA

Figure 1 shows a plot of the work functions of the metallic *sp* valent elements from the 3<sup>rd</sup> through 6<sup>th</sup> rows of the periodic table and the trivalent rare earth elements of the group *rey*. The Si bulk work function,  $\phi^*$ , is also shown. The *sp* valent and rare earth metals have been previously evaluated.<sup>2</sup> It was shown that the rare earth elements could be subdivided into three groups according to their total angular momentum, *L*. The rare earths, including Sc and Y, are grouped as *L* = 0 [*reα* (Sc, Y, La, Gd, Lu)], *L* = 3 or 6 [(*reβ* (Ce, Nd, Pm, Tb, Ho, Er) and *L* = 5 [*rey* (Pr, Sm, Dy, Tm)]. From the strong linear correlation between  $\phi_m$  and  $\mu_\alpha$  for each group and the common slope it was argued that "good" polycrystalline surfaces have no net surface dipole. The consequence of this assertion is that the work function corresponds exactly to the bulk chemical potential of the metal as measured relative to the vacuum level. The present work attempts to extend that work to include the transition metals and metal silicide compounds.

Figure 2 shows the work functions of the 3*d* transition metals as a function of the atomic chemical potential assuming that only the two valence



$s$  electrons contribute to the polarizability. This is assuming  $n = 2$  in Equation 4. Most of the experimental values for polycrystalline work functions are drawn from Michaelson. Only values for Ti and Co are taken from a more recent reference.<sup>13</sup> Three values shown for Mn are determined by different techniques. Mn(P) was measured by the photoelectric effect and is the value cited by Michaelson. Mn(T) was determined by thermionic emission<sup>14</sup> and Mn(F) was determined by field-emission retarding-potential (FERP) technique.<sup>13</sup> While 0.1 eV error bars are shown for all elements the actual error for Mn(P) is  $\pm 0.2$  eV and that for Mn(F) was only  $\pm 0.04$  eV. The elements are grouped as early transition metals, *etm*, late transition metals, *ltm*, and the metals which have full  $d$  shells in the atomic ground state. These are denoted as transition metals with 10 electrons, *tm10*. While each of the three subgroups have a common slope it is significantly greater than that of the  $sp$  valent metals. Representing the  $sp$  valent metals the line for the IIA/IIB metals is shown as a dashed line. Classification of Mn is problematic as the different values each coincide with a different group. Mn has a half filled  $d$  shell which results in a contraction of the average radius of the  $d$  electrons relative to the other  $3d$  metals. This allows that it might well behave as a group II element and is consistent with its chemical behavior. Alternatively, the Mn(F) value groups with the *tm10* elements. Again, the half filled  $d$  shell could be offered as a reason for this behavior. Theoretical evaluation of the work functions of the transition metals favor selection of the highest value, Mn(P). This selection is consistent with other trends discussed later.

Figures 3 and 4 illustrate the work function variations of the  $4d$  and  $5d$  metals. As in Figure 2 the computation of the atomic chemical potential assumes  $n = 2$ . In each case the elements may be grouped as *etms*, *ltms* and

*tm10s*. They all have slopes greater than that of the *sp* valent metals and, aside from the IIB metals, work functions greater than divalent metals with the same  $\mu_\alpha$ . Exceptional elements are Y, La and Au. Y and La behave as rare earths rather than transition metals. The value for Au has been reproduced in numerous investigations and its high value relative to Hg is rationalized later. In Figure 3 a value of  $\phi = 4.82$  eV is extrapolated for Tc. This is in good agreement with the value of  $4.88 \pm 0.05$  eV derived by correlation with the Pauling electronegativity and the exchange current for electrolytic hydrogen evolution on Tc.<sup>15</sup> Tc is identified as an *etm* because it forms chemical compound in a high valence state as does Re. Mn is unique in the VIIA metals in predominantly adopting the +2 chemical valence state which is characteristic of the *3d ltns*.

For the rare earth elements it was shown that the assumption of  $n = 3$  for the trivalent elements brought the *rey* elements into alignment with the IIB elements as shown in Figure 1.<sup>2</sup> The *rea* elements, including Sc, Y, and La fell on the IIA/IIB line under the assumption of  $n = 3$ . Of these Sc and Y have no *f* electrons to contribute to the polarizability assuming only valence electrons make a significant contribution to  $\alpha$ . Following this observation, if the transition metals are to be made to adopt the slope of the metallic *sp* valent and rare earth elements, an effective  $n$  value greater than two must be assumed for each metal other than the IIIA and IIB elements. The minimal adjustment would modify  $\mu_\alpha$  such that each  $\phi_m$  fell within experimental error ( $\pm 0.1$  eV) of the IIA/IIB line. The motivation for such an adjustment is to obtain a good value of  $\eta_\alpha = \mu_\alpha/e$ . Computation of silicide work functions is sensitive to value of  $\eta_\alpha$  assumed for the metal.

The results of computing the effective number of electrons,  $n_{eff}$ , contributing to  $\alpha$  are shown in Figure 5. The elements clearly fall out into the

*etm*, *ltm*, and *tm10* groups. For the *etms* the *3d* and *5d* metals cluster along the lower edge of the rhombus with the *4d* metals at the upper edge. For the *ltms* the *5d* metals move to the upper edge of the rhombus with the *4d* metals. For the *tm10* metals the IIB metals all have  $n_{\text{eff}}$  very close to 2. Pd(2.34) and Au(2.85) are close to the upper edge of the rhombus consistent with the behavior of the *4d* and *5d* *ltms*. The preferred chemical valences of these elements are +2 and +3, respectively. Cu and Ag both have  $n_{\text{eff}}$  close to 2. Cu prefers a +2 valence state, Ag adopts only a +1 chemical valence. Noting that Au falls almost exactly on the IA line for  $n_{\text{eff}} = 2$  and does not group with Hg in Figure 4, the IB metal  $n_{\text{eff}}$ s were all adjusted to place them on the IA line instead of the IIA/IIB line.

To calculate  $\eta_{\alpha}$  for each atom,  $n_{\text{eff}}$  was taken to be the value at the rhombus edge closest to the exact  $n_{\text{eff}}$  for each element, excepting the IB metals. This was done in an attempt to minimize the effect of experimental uncertainty in  $\phi$  on the trends in  $\mu_{\alpha}$ . The rhombuses are identical, shifting down one electron and three to the left as one progress from left to right. The slope of the edge is 0.457. Table I contains a list of the work functions, atomic chemical potentials, hardnesses and effective number of electrons of the metallic elements from rows three through six of the periodic table. These values will be used to compute the work functions of the transition metal and rare earth silicides.

Values for silicide work functions are drawn from a search of the literature up to the end of 1998. They are given in Table II with the theoretical values derived from Equation 6. The difference between the average charge transfer (ACT) and geometric mean work functions computed using  $\phi^* = 4.66$  eV are also given for each silicide. Using the surface work function  $\phi(\text{Si}) = 4.85$  eV as tabulated by Michaelson would increase the error

by an average 0.1 eV. The correlation between the experimental and ACT work function,  $\phi_{ACT}$ , as computed by Equation 6 is illustrated in Figure 6. Solid symbols denote values measured on bulk samples. Open symbols denote values for thin film samples. Circles are used for metallic silicides and squares for semiconducting silicides. The horizontal line in Figure 6 is drawn at the silicon bulk work function  $\phi^*$ . In some cases, multiple values for a single silicide are connected by a vertical line to aid in their identification. Only the endpoints correspond to the identified silicide. Using the geometric mean work function would result in a qualitatively similar figure with the horizontal axis compressed. The difference between the two models increases at  $|\phi_m - \phi^*|$  increases. The largest error occurs for the rare earth silicides where the geometric mean work function is 0.15-0.20 eV larger than the ACT work functions.

The slope of the chain and dashed lines was determined by a fit through two amorphous Er silicides and one crystalline silicide as prepared by one group.<sup>16</sup> The work function increases linearly as a function of the ACT work function as the Si content increases. The chain line fit through the Er silicides fits the Y, Sm, and Yb silicides as well. The only outlier is  $TbSi_{1.7}$ . A similar fit can be made to the transition metals for which  $\phi_m \leq \phi^*$ . The only outlier in this group is the value for  $HfSi_2$ . Metals for which  $\phi_m \geq \phi^*$  more closely follow the prediction of the ACT model with a tendency for the experimental work function to fall below the predicted value. This contrasts with the tendency toward larger experimental values for  $\phi_m \leq \phi^*$ .

## DISCUSSION

It is clear from Figures 2 through 4 that there is a strong correlation between the polycrystalline work function and  $\mu_\alpha$  for the transition metals of

each row of the periodic table. Only the values for La, Ti, and Co have been reduced from the values cited by Michaelson.<sup>2,13</sup> Within each row the elements can be classified as early transition metals, late transition metals and transition metals with 10 *d* electrons in the atomic ground state. With the exception of Sc the IIIA rare earths do not group as *etms*. Excluding the IIIA metals, the strong linear correlation between  $\phi_m$  and  $\mu_\alpha$  for the transition metals suggests that, like the metallic *sp* valent and the rare earth elements, the net surface dipole of good polycrystalline samples is zero. The fact that the slope of the fit to the transition metals is approximately twice that of the other metallic elements is interpreted to mean that both *s* and *d* electrons contribute to the total atomic polarizability. To evaluate the effective number of electrons contributing to the atomic polarizability it is necessary assume correct values for the atomic chemical potential. Guided by the observation that the trivalent IIIA rare earth elements fall on the IIA/IIB line for  $n = 3$  the effective number of electrons required to shift the transition metals to the IIA/IIB line was computed. The resulting values of  $n_{eff}$ , when grouped according to *etm*, *ltm* and *tm10*, demonstrated periodic behavior.

For the IB metals  $n_{eff}$  was adjusted to have  $\phi_m$  fall on the IA line. The only validity check for this assumption would be the effect on the computed work function of the copper silicide. Unfortunately, Cu and Si work functions differ by only 0.01 eV and the effect of changing  $n_{eff}$  is inconsequential. Despite its regular behavior the consistency in the behavior in  $n_{eff}$  does not, in and of itself, justify the assumption that the transition metal work functions should correlate with the IIA/IIB line in a  $\phi_m$  vs  $\mu_\alpha$  plot. In fact, use of  $n_{eff} = 2$  for all of the transition metals would not appreciably alter the silicide results. The correction is imposed because it is physically

intuitive that  $n_{\text{eff}}$  should vary in qualitatively the observed manner and is consistent with the correct application of Equation 6.

The ACT model allows the classification of transition metal silicides into three groups. This separation is not a direct consequence of the ACT model. For Er and Ti silicides with  $\phi_m \leq \phi^*$  it is seen that  $\phi_m$  varies linearly with  $\phi_{\text{ACT}}$  as a function of metal to silicon ratio. The increased slope relative to the ACT line suggests the existence of a surface dipole. The rare earth silicides all have the  $\text{AlB}_2$  crystal structure (or a close variation) and thin films formed by the reaction of the metal and a silicon substrate invariably present the basal plane at the surface. However, two amorphous Er silicide help define the linear correlation and should have substantially larger smoothing dipoles than planar crystalline faces. For the *etm* silicides fit by the dashed lines both thin film and bulk samples are represented as well as several different crystal structures. The assumption of a surface dipole which varies linearly from positive to negative with increasing ACT work function would be hard to justify in terms of any simple mechanism.

It is difficult to explain the behavior of the  $\phi_m \leq \phi^*$  metals in terms of either bulk or surface dipole effects. Perhaps in these compounds one observes an intrinsic surface chemical potential. At the surface of an elemental metal all of the electrons are free to redistribute as required to minimize the surface energy. In a purely covalent element, surface electrons localize in directed dangling bond states or adjacent surface atoms relax to promote the formation of directed surface bonds. As the stoichiometry of a polycrystalline silicide becomes Si rich an increasing number of Si atoms will be present at a surface. The character of the surface electrons will change from delocalized to localized. This will inhibit the tendency to the surface to form spreading or smoothing dipoles as characteristic of a metal surface. For  $\phi_m <$

intuitive that  $n_{\text{eff}}$  should vary in qualitatively the observed manner and is consistent with the correct application of Equation 6.

The ACT model allows the classification of transition metal silicides into three groups. This separation is not a direct consequence of the ACT model. For Er and Ti silicides with  $\phi_m \leq \phi^*$  it is seen that  $\phi_m$  varies linearly with  $\phi_{\text{ACT}}$  as a function of metal to silicon ratio. The increased slope relative to the ACT line suggests the existence of a surface dipole. The rare earth silicides all have the  $\text{AlB}_2$  crystal structure (or a close variation) and thin films formed by the reaction of the metal and a silicon substrate invariably present the basal plane at the surface. However, two amorphous Er silicide help define the linear correlation and should have substantially larger smoothing dipoles than planar crystalline faces. For the *etm* silicides fit by the dashed lines both thin film and bulk samples are represented as well as several different crystal structures. The assumption of a surface dipole which varies linearly from positive to negative with increasing ACT work function would be hard to justify in terms of any simple mechanism.

It is difficult to explain the behavior of the  $\phi_m \leq \phi^*$  metals in terms of either bulk or surface dipole effects. Perhaps in these compounds one observes an intrinsic surface chemical potential. At the surface of an elemental metal all of the electrons are free to redistribute as required to minimize the surface energy. In a purely covalent element, surface electrons localize in directed dangling bond states or adjacent surface atoms relax to promote the formation of directed surface bonds. As the stoichiometry of a polycrystalline silicide becomes Si rich an increasing number of Si atoms will be present at a surface. The character of the surface electrons will change from delocalized to localized. This will inhibit the tendency to the surface to form spreading or smoothing dipoles as characteristic of a metal surface. For  $\phi_m <$

$\phi^*$  bond charge will flow from the metal to the silicon atoms and the surface chemical potential should be dominated by charge localization around the silicon atoms. In the case where  $\phi^* < \phi_m$  bond charge flows away from the silicon atoms emptying the localized states in favor of metallic states. Only those silicides which favor the filling of metallic states correlate directly with the ACT prediction.

From Figure 6 it can also be seen that for  $\phi_m < \phi^*$  experimental work functions tend to be high within each of the two groups while for  $\phi_m > \phi^*$  they tend to be low with respect to the ACT prediction. When annealed silicides have a tendency to become silicon rich at the surface.<sup>17</sup> If the work function measures the surface composition then the errors on either side of  $\phi^*$  are typically consistent silicon surface enrichment. Exceptions are low and high values of  $\text{CrSi}_2$  and  $\text{PdSi}_2$ , respectively. Given that most silicides are well behaved, these examples may simply indicate that experimental artifacts are the exception rather than the rule. It is also surprising that there does not seem to be more evidence for face dependent work functions in the silicides.

The equations for the surface work functions of the rare earth and low work function transition metal silicide groups are

$$\phi(\text{reSi}) = 2.457(\phi_{\text{ACT}} - 3.469) + 3.469 \quad (7)$$

$$\phi(\text{tmSi}) = 2.457(\phi_{\text{ACT}} - 4.483) + 4.483 \quad (8)$$

For the purposes of predicting silicide work functions these equations are clearly more useful than either the ACT model alone or the model of the geometric mean. Equation 7 is also likely to be valid for predicting the work functions of the IA and IIA silicides work functions for which no experimental data was found. The break in the data for  $\phi_m = \phi^*$  is consistent with the identification of the metal work functions as representing the bulk chemical potentials of the metals and Si. Use of the ACT model does provide



much better agreement between experiment and theory for the high work function metals than does the model of the geometric mean.

## SUMMARY

Transition metal work functions have been evaluated under the assumption that a good polycrystalline work function is consistent with a zero net surface dipole. The assertion of a zero surface dipole follows from the strong linear correlation between bulk and atomic properties. By forcing the behavior of the transition metals to be similar to the behavior of the metallic *sp* valent and rare earth elements the effective number of polarizable electrons may be derived. This in turn allows the computation of the atomic hardness of the transition metal elements.

Asserting that the polycrystalline work function is a measure of the bulk chemical potential the atomic hardnesses are used to compute the bulk chemical potentials of metal silicide compounds using an average charge transfer model. Comparison of the computed and experimental work functions shows that the silicides separate as rare earths and transition metals whose work function is less than that of Si. Separation of the silicides into groups with similar linear correlations suggests the postulate of an intrinsic surface chemical potential for compounds formed of a metallic element with a covalent element. Directional bonds formed at silicon containing surfaces limit the free redistribution of electronic charge. In low work function metals the surface work function is strongly affected by electron localization about the silicon atoms. While only metal silicides were investigated in the present work similar results are expected for metal germanides.

## ACKNOWLEDGEMENTS

Sandia is a multiprogram laboratory operated by Sandia Corporation, a Lockheed Martin Company, for the United States Department of Energy under Contract DE-AC04-94AL85000. The author would like to thank Dr. A Baca for critically reading the manuscript.

## REFERENCES

- <sup>1</sup> H. B. Michaelson, *J. Appl. Phys.* **48**, 4729 (1977).
- <sup>2</sup> T. J. Drummond, *J. Appl. Phys.* **0**, 0 (1999).
- <sup>3</sup> R. Smoluchowski, *Phys. Rev.* **60**, 661 (1941).
- <sup>4</sup> L. Komorowski, *Chem. Phys.* **114**, 55 (1987).
- <sup>5</sup> R. G. Parr, R. A. Donnelly, M. Levy, and W. E. Palke, *J. Chem. Phys.* **68**, 3801 (1978).
- <sup>6</sup> N. K. Ray, L. Samuels, and R. G. Parr, *J. Chem. Phys.* **70**, 3680 (1979).
- <sup>7</sup> J. K. Nagle, *J. Am. Chem. Soc.* **112**, 4741 (1990).
- <sup>8</sup> J. L. Freeouf, *Sol. St. Commun.* **33**, 1059 (1980).
- <sup>9</sup> F. J. Himpsel, G. Hollinger, and R. A. Pollak, *Phys. Rev. B* **28**, 7014 (1983).
- <sup>10</sup> W. Mönch, *Appl. Surf. Sci.* **117/118**, 380 (1997).
- <sup>11</sup> T. J. Drummond, *Phys. Rev. B* **59** (1999).
- <sup>12</sup> W. Walukiewicz, *Phys. Rev. B* **37**, 4760 (1988).
- <sup>13</sup> Y. Fukuda, W. T. Elam, and R. L. Park, *Phys. Rev. B* **16**, 3322 (1977).
- <sup>14</sup> T. M. Lifshits, and A. L. Musatov, *Electron and Ion Emission*, In Handbook of Physical Quantities, I. S. Grigoriev, and E. Z. Meilikhov (Eds.) (Boca Raton: CRC Press) 1997.
- <sup>15</sup> S. Trasatti, *Surf. Sci.* **32**, 735 (1972).
- <sup>16</sup> P. Wetzal, L. Haderbache, C. Pirri, J. C. Peruchetti, D. Bolmont, and G. Gewinner, *Phys. Rev. B* **43**, 6620 (1991).

- <sup>17</sup> F. M. d'Heurle, *Journal de Physique IV* **6**, 29 (1996).
- <sup>18</sup> E. Bucher, S. Schultz, M. C. Lux-Steiner, P. Munz, U. Gubler, and F. Greuter, *Applied Physics A* **40**, 71 (1986).
- <sup>19</sup> G. V. Samsonov, L. N. Okhremchuk, N. F. Podgrushko, I. A. Podchernyaeva, and V. S. Fomenko, *Inorganic Materials* **12**, 720 (1976).
- <sup>20</sup> P. Wetzell, C. Pirri, J. C. Peruchetti, D. Bolmont, and G. Gewinner, *Phys. Rev. B* **35**, 5880 (1987).
- <sup>21</sup> S. Kennou, and T. A. Nguyen Tan, *Surf. Sci. Lett.* **248**, L255 (1991).
- <sup>22</sup> E. Gullikson, A. P. Mills Jr., and J. M. Phillips, *Surf. Sci.* **195**, L150 (1988).
- <sup>23</sup> C. Pirri, J. C. Peruchetti, D. Bolmont, and G. Gewinner, *Phys. Rev. B* **33**, 4108 (1986).
- <sup>24</sup> Y.-J. Chang, and J. L. Erskine, *J. Vac. Sci. Technol. A* **1**, 1193 (1983).
- <sup>25</sup> A. Taleb-Ibrahimi, V. Mercier, C. A. Sébenne, D. Bolmont, and P. Chen, *Surf. Sci.* **152/153**, 1228 (1985).
- <sup>26</sup> R. Baptist, A. Pellissier, and G. Chauvet, *Sol. St. Commun.* **68**, 555 (1988).
- <sup>27</sup> T. Yamauchi, H. Kitamura, N. Wakai, S. Zaima, Y. Koide, and Y. Yasuda, *J. Vac. Sci. Technol. A* **11**, 2619 (1993).
- <sup>28</sup> M. Azizan, T. A. Nguyen Tan, R. C. Cinti, G. Chauvet, and R. Baptist, *Sol. St. Commun.* **54**, 895 (1985).
- <sup>29</sup> T. T. A. Nguyen, and R. C. Cinti, *Journal de Physique* **45**, 435 (1984).
- <sup>30</sup> T. V. Krachino, M. V. Kuz'min, M. V. Loginov, and M. A. Mittsev, *Phys. Sol. St.* **40**, 1758 (1998).

- <sup>31</sup> J.-Y. Veuillen, S. Kennou, and T. A. Nguyen Tan, *Sol. St. Commun.* **79**, 795 (1991).
- <sup>32</sup> L. Stauffer, C. Pirri, P. Wetzell, A. Mharchi, P. Paki, D. Bolmont, and G. Gewinner, *Phys. Rev. B* **46**, 13201 (1992).
- <sup>33</sup> A. Siokou, S. Kennou, and S. Ladas, *Surf. Sci.* **331-333**, 580 (1995).
- <sup>34</sup> J. Y. Veuillen, T. A. Nguyen Tan, S. Ladas, and S. Kennou, *Phys. Rev. B* **52**, 10796 (1995).
- <sup>35</sup> T. V. Krachino, M. V. Kuz'min, M. V. Loginov, and M. A. Mittsev, *Phys. Sol. St.* **39**, 1493 (1997).
- <sup>36</sup> T. A. Nguyen Tan, M. Azizan, and J. Derrien, *Surf. Sci.* **189/190**, 339 (1987).
- <sup>37</sup> M. Azizan, T. A. Nguyen Tan, R. Cinti, R. Baptist, and G. Chauvet, *Surf. Sci.* **178**, 17 (1986).
- <sup>38</sup> S.-L. Weng, *Phys. Rev. B* **29**, 2363 (1984).
- <sup>39</sup> A. Siokou, S. Kennou, S. Ladas, T. A. Nguyen Tan, and J.-Y. Veuillen, *Surf. Sci.* **352-354**, 628 (1996).

Element	$\alpha_z$	$n_{\text{eff}}$	$n_{\alpha} (10^{18} \text{ F}^{-1})$	$\mu_{\alpha} (\text{V})$	$\phi (\text{eV})$
Na	23.6	1	31.3	5.02	2.75
Mg	10.6	2	51.5	8.26	3.66
Al	8.34	3	63.9	10.24	4.28
Si	5.38	4	81.4	13.05	<u>4.66</u>
K	43.4	1	25.6	4.10	2.30
Ca	22.8	2	39.9	6.40	2.87
Sc	17.8	3	49.6	7.95	$3.5 \pm 0.15$
Ti	14.6	3.34	55.0	9.61	$3.96 \pm 0.04$
V	12.4	3.69	60.0	9.61	$4.3 \pm 0.1$
Cr	11.6	4.03	63.2	10.12	$4.5 \pm 0.15$
Mn	9.4	2.34	56.6	9.06	$4.1 \pm 0.2$
Fe	8.4	2.69	61.5	9.84	$4.5 \pm 0.15$
Co	7.5	3.03	66.4	10.64	$4.92 \pm 0.04$
Ni	6.8	3.37	71.1	11.39	$5.15 \pm 0.1$
Cu	6.1	1.58	57.3	9.18	$4.65 \pm 0.05$
Zn	7.1	2	58.9	9.44	4.33
Ga	8.12	3	64.5	10.33	4.2
Rb	47.3	1	24.9	3.98	2.261
Sr	27.6	2	37.5	6.00	2.64
Y	22.7	3	45.8	7.33	$3.1 \pm 0.15$
Zr	17.9	4	54.5	8.74	$4.05 \pm 0.1$
Nb	15.7	4.69	60.1	9.62	$4.3 \pm 0.15$
Mo	12.8	5.03	65.8	10.54	$4.6 \pm 0.15$
Tc	11.4	5.37	69.9	11.20	<u>4.82</u>
Ru	9.6	3.69	65.3	10.46	4.71
Rh	8.6	4.03	69.8	11.18	4.98
Pd	4.8	2.34	70.8	11.34	5.12
Ag	7.2	1.39	51.9	8.32	4.26
Cd	7.2	2	58.6	9.39	4.22
In	9.1	3	62.1	9.95	4.12
Sn	7.7	4	72.2	11.58	4.3
Sb	6.6	5	81.9	13.13	4.55
Cs	59.6	1	23.0	3.69	2.14
Ba	39.7	2	33.2	5.32	2.3
La	31.1	3	41.2	6.60	2.91
Ce	29.6	3	41.9	6.71	$2.9 \pm 0.2$
Pr	28.2	3	42.6	6.82	2.62
Nd	31.4	3	41.1	6.58	2.83
Pm	30.1	3	41.7	6.68	<u>2.89</u>
Sm	28.8	3	42.3	6.77	$2.7 \pm 0.3$

Eu	27.7	2	37.4	6.00	2.5 ± 0.3
Gd	23.5	3	45.3	7.25	3.1 ± 0.15
Tb	25.5	3	44.0	7.06	3.0
Dy	24.5	3	44.6	7.15	2.78
Ho	23.6	3	45.2	7.24	3.03
Er	22.7	3	45.8	7.33	3.09
Tm	21.8	3	46.4	7.43	2.94
Yb	21.0	2	41.0	6.58	2.70
Lu	21.9	3	46.3	7.42	3.3
Hf	16.2	3.34	53.1	8.51	3.9 ± 0.1
Ta	13.1	3.69	58.9	9.43	4.25
W	11.1	4.03	64.1	10.27	4.55
Re	9.7	4.37	68.9	11.04	4.96
Os	8.5	2.69	61.2	9.81	4.83
Ir	7.6	3.03	66.1	10.59	5.27
Pt	6.5	3.37	72.2	11.57	5.65 ± 0.1
Au	5.8	2	63.0	10.10	5.1 ± 0.1
Hg	5.7	2	63.4	10.16	4.49
Tl	7.5	3	66.2	10.61	3.84
Pb	6.8	4	75.3	12.07	4.25
Bi	7.4	5	78.9	12.64	4.22

Table I

Values for the atomic polarizability, effective electron density, atomic hardness, atomic chemical potential, and experimental work function are tabulated for the metallic elements in rows three through six of the periodic table. Polarizabilities are from Nagle<sup>7</sup> and work functions from Michaelson, Fukuda et al., and Drummond.<sup>1,2,13</sup> Underlined work function values for Si, Tc, and Pm are estimates.

Silicide	experimental	ACT	ACT - mean	reference
	$\phi$ (eV)	$\phi$ (eV)	$\Delta\phi$ (eV)	
TiSi <sub>2</sub>	4.53 (b)	4.36	0.05	18
	4.10 (b)			19
TiSi	3.99 (b)	4.24	0.05	19
Ti <sub>5</sub> Si <sub>3</sub>	3.71 (b)	4.16	0.05	19
VSi <sub>2</sub>	4.63 (b)	4.51	0.02	18
CrSi <sub>2</sub> (s)	4.85 (f)	4.60	0.01	20
	4.32 (b)			18
CrSi	4.82 (f)	4.57	0.01	20
FeSi <sub>2</sub> (s)	4.65 (f)	4.60	0.01	21
CoSi <sub>2</sub>	4.62 (f)	4.76	-0.01	22
	4.75 (f)			23
	4.77 (b)			18
NiSi	4.84 (f)	4.92	-0.02	24
Ni <sub>2</sub> Si	4.94 (f)	5.00	-0.02	24
	4.96 (b)			18
Cu <sub>3</sub> Si	4.76 (f)	4.65	0.00	25
YSi <sub>1.7</sub>	4.51 (f)	3.85	0.14	26
ZrSi <sub>2</sub>	4.30 (f)	4.40	0.05	27
	4.57 (b)			19
NbSi <sub>2</sub>	4.75 (f)	4.51	0.02	28
MoSi <sub>2</sub>	4.60 (f)	4.64	0.00	29
	4.82 (b)			18



Pd <sub>2</sub> Si	5.00 (b)	4.98	-0.02	18
	5.40 (f)			8
SmSi <sub>1.7</sub>	4.10 (f)	3.72	0.18	30
TbSi <sub>1.7</sub>	4.65 (f)	3.79	0.16	31
ErSi <sub>1.7</sub>	4.40 (f)	3.85	0.14	16
	4.75 (f)			32
	4.80 (f)			33
	5.40 (f)			34
ErSi <sub>0.82</sub> (a)	3.75 (f)	3.58	0.13	16
ErSi <sub>0.25</sub> (a)	3.00 (f)	3.28	0.07	16
YbSi <sub>2</sub>	3.95 (f)	3.68	0.20	35
HfSi <sub>2</sub>	4.51 (b)	4.33	0.06	19
TaSi <sub>2</sub>	4.75 (b)	4.49	0.03	36
WSi <sub>2</sub>	4.88 (b)	4.62	0.01	18
	4.70 (f)			37
	5.20 (f)			38
ReSi <sub>2</sub> (s)	4.70 (f)	4.77	-0.01	39
OsSi <sub>1.8</sub> (s)	4.75 (f)	4.73	-0.01	18
IrSi	5.08 (b)	5.00	-0.04	18
IrSi <sub>3</sub> (s)	4.68 (b)	4.84	-0.03	18
PtSi	4.86 (b)	5.05	-0.04	18
	4.98 (f)			8
Pt <sub>2</sub> Si	5.17 (b)	5.17	-0.03	18

Table II

Experimental work functions for metal silicide are tabulated and distinguished as measurements from bulk (b) and thin film (f) samples. Semiconducting silicides are marked (s) and amorphous silicides are marked (a). Computed values for the ACT work function follow from Equation 6. The difference  $\Delta\phi$  is between the ACT work function and the geometric mean work function computed from Equation 5. References are cited for the experimental work functions.

## FIGURE CAPTIONS

Figure 1) Metal work functions for the metallic *sp* valent and the *rey* rare earth elements plotted as a function of the atomic chemical potential,  $\mu_a$ . Each fit to a group has the same slope. The group IIB and IIIB elements were not included in the fits to the IIA and *rey* elements.

Figure 2) Work functions of the *3d* transition metals as a function of the atomic chemical potential computed for  $n = 2$ . Each group *etm*, *ltm*, and *tm10* is fit to a line of the same slope. The fit to the IIA/IIB elements is shown as a dashed line. Sc is unique in correlating both as an early transition metal and as a rare earth element. The preferred value for Mn is the highest value grouping with the late transition metals.

Figure 3) Work functions of the *4d* transition metals as a function of the atomic chemical potential computed for  $n = 2$ . Each group *etm*, *ltm*, and *tm10* is fit to a line of the same slope. The fit to the IIA/IIB elements is shown as a dashed line.

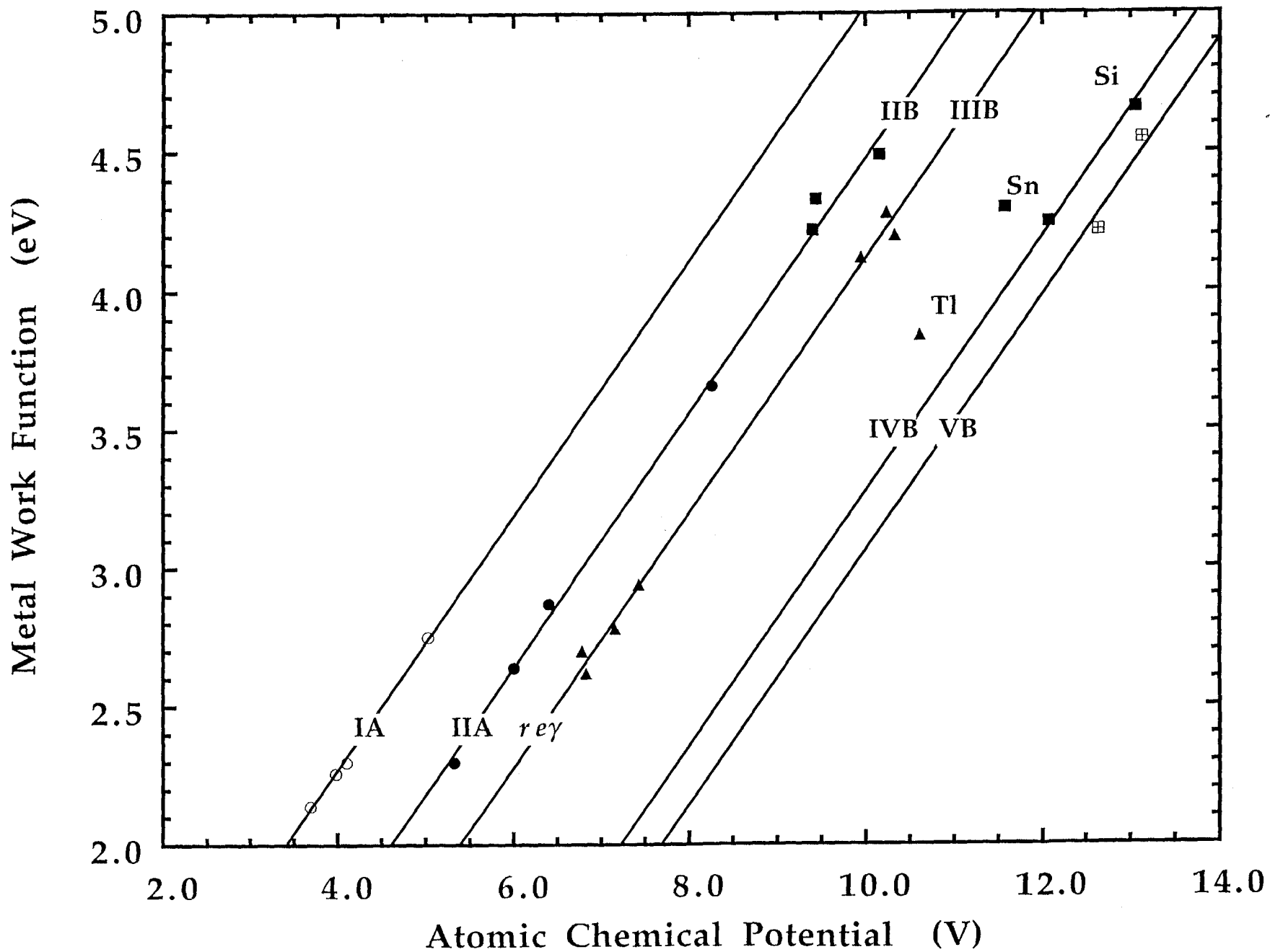
Figure 4) Work functions of the *5d* transition metals as a function of the atomic chemical potential computed for  $n = 2$ . Each group *etm*, *ltm*, and *tm10* is fit to a line of the same slope. The fit to the IIA/IIB elements is shown as a dashed line. Au does not classify as either a *tm10* according to this

representation. Au, a IB element, does fall on the IA line which is not shown. It is the only IB element to do so for  $n = 2$ .

Figure 5) Assuming that each transition metal element work function should fall on the IIA/IIB line the effective number of polarizable electrons is calculated and plotted as a function of the total number of  $d$  electrons associated with the element. Each rhombus is identical in size and shape. To allow for uncertainty in the experimental work functions the effective number of electrons for an element is estimated as the value at the nearest rhombus edge. IB metals were adjusted to correlate with the IA line rather than the IIA/IIB line.

Figure 6) Experimental silicide work functions are plotted as a function of the average charge transfer work function. The horizontal line locates the bulk chemical potential of Si,  $\phi^*$ . The chain line is a fit to the Er silicides and passes close to all of the *re* silicides. The dashed line has the same slope and describes the behavior of the *tm* silicides with  $\phi_m < \phi^*$ .

Figure 1



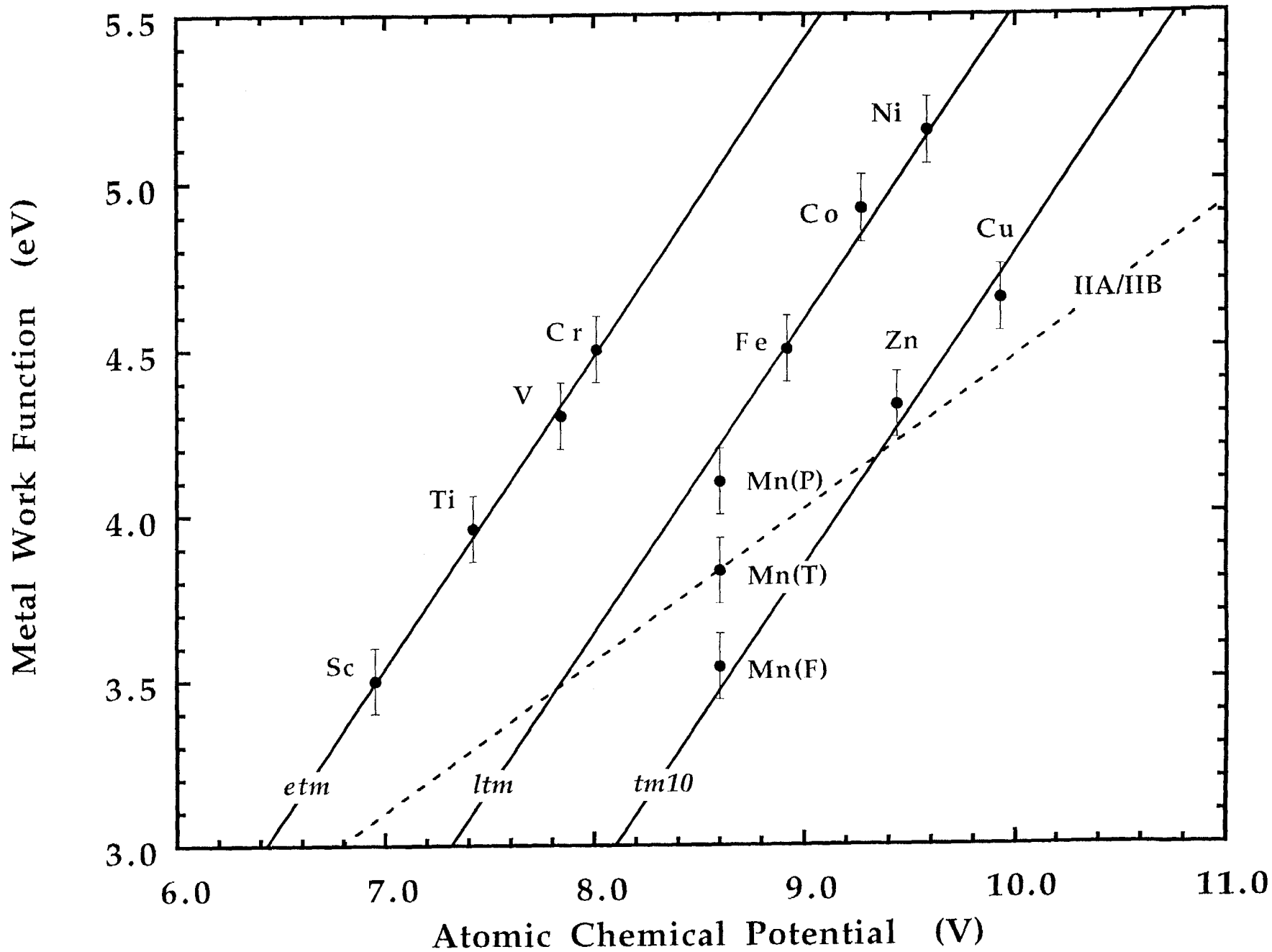


Figure 2

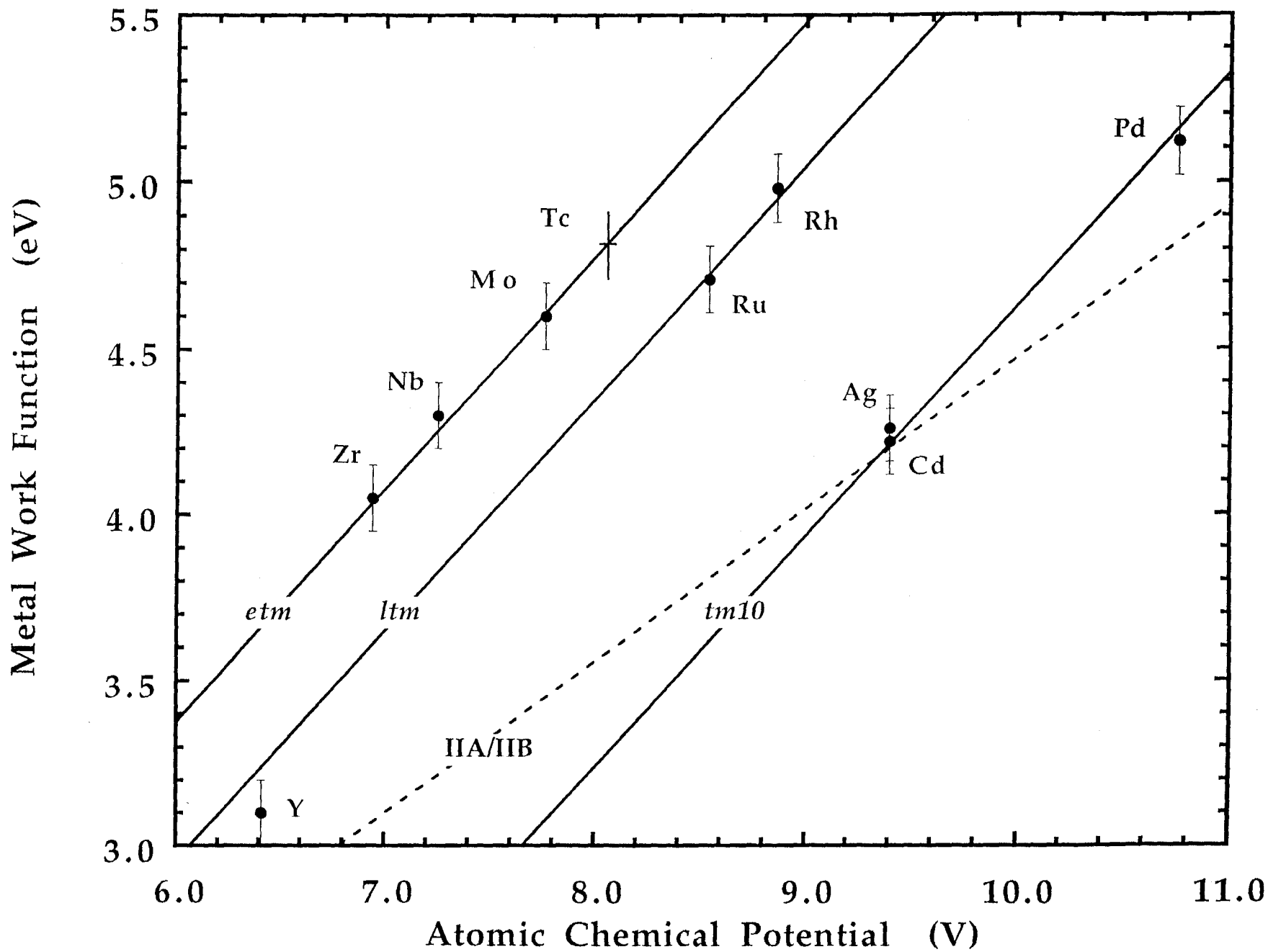
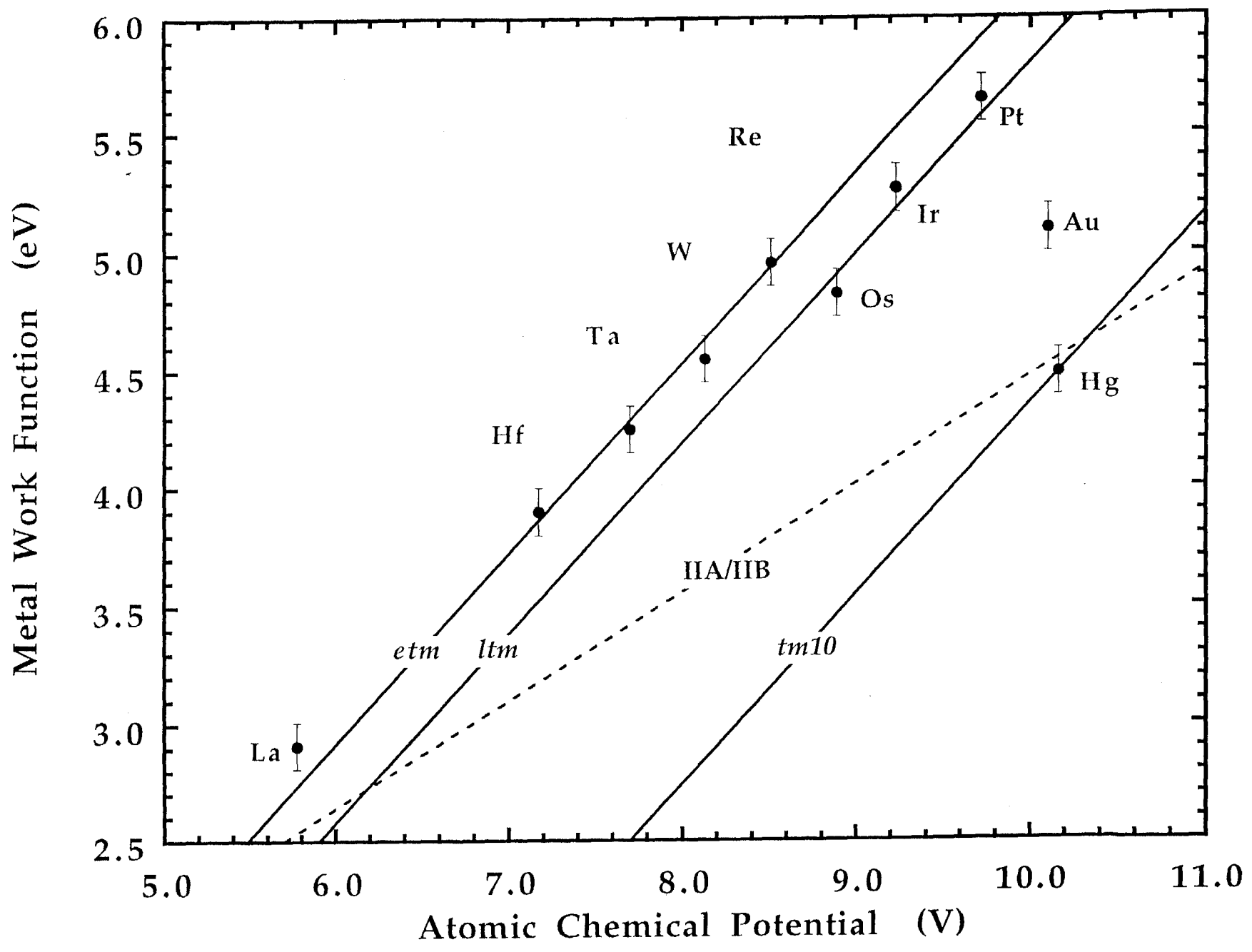


Figure 3

Figure 4





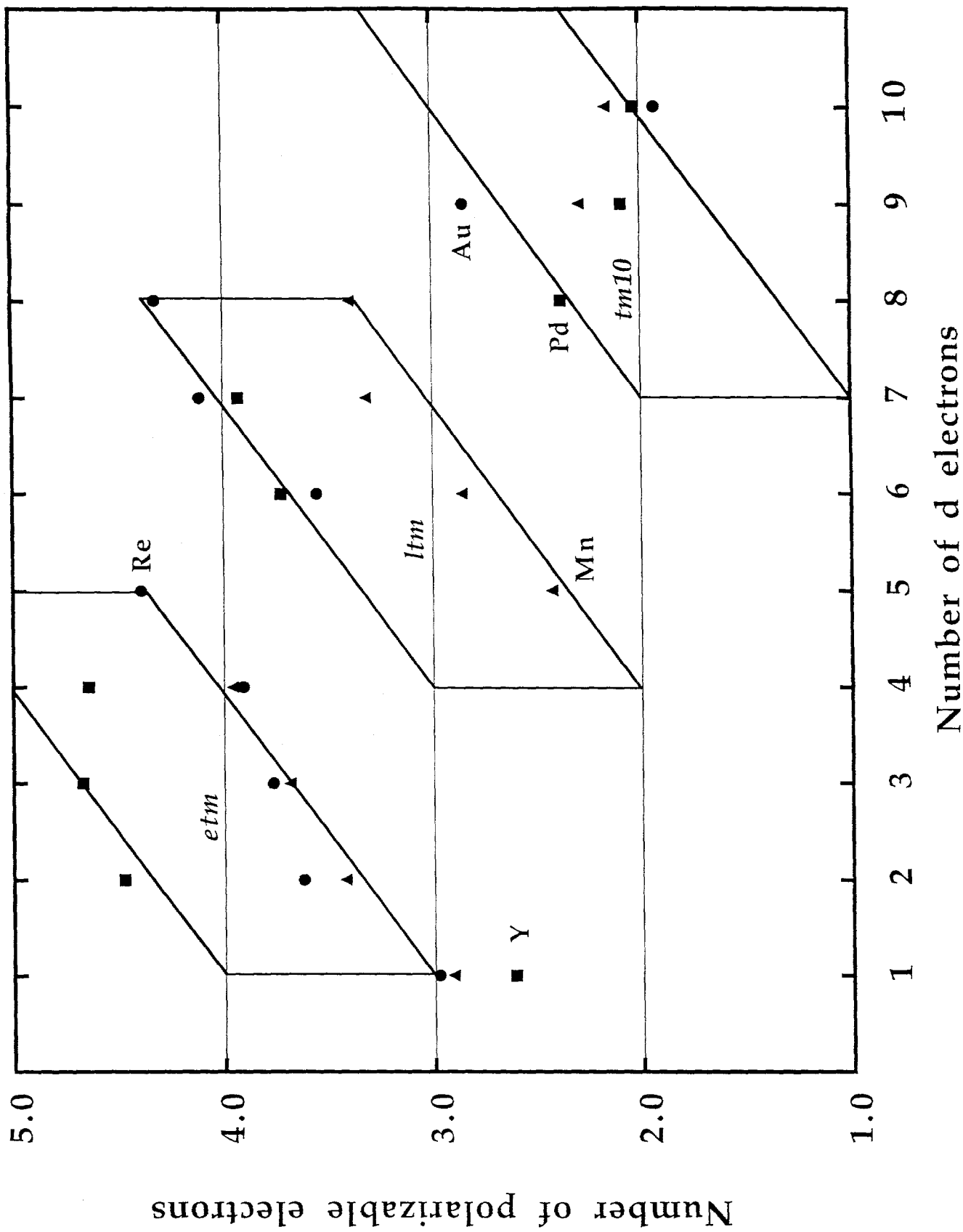


Figure 5

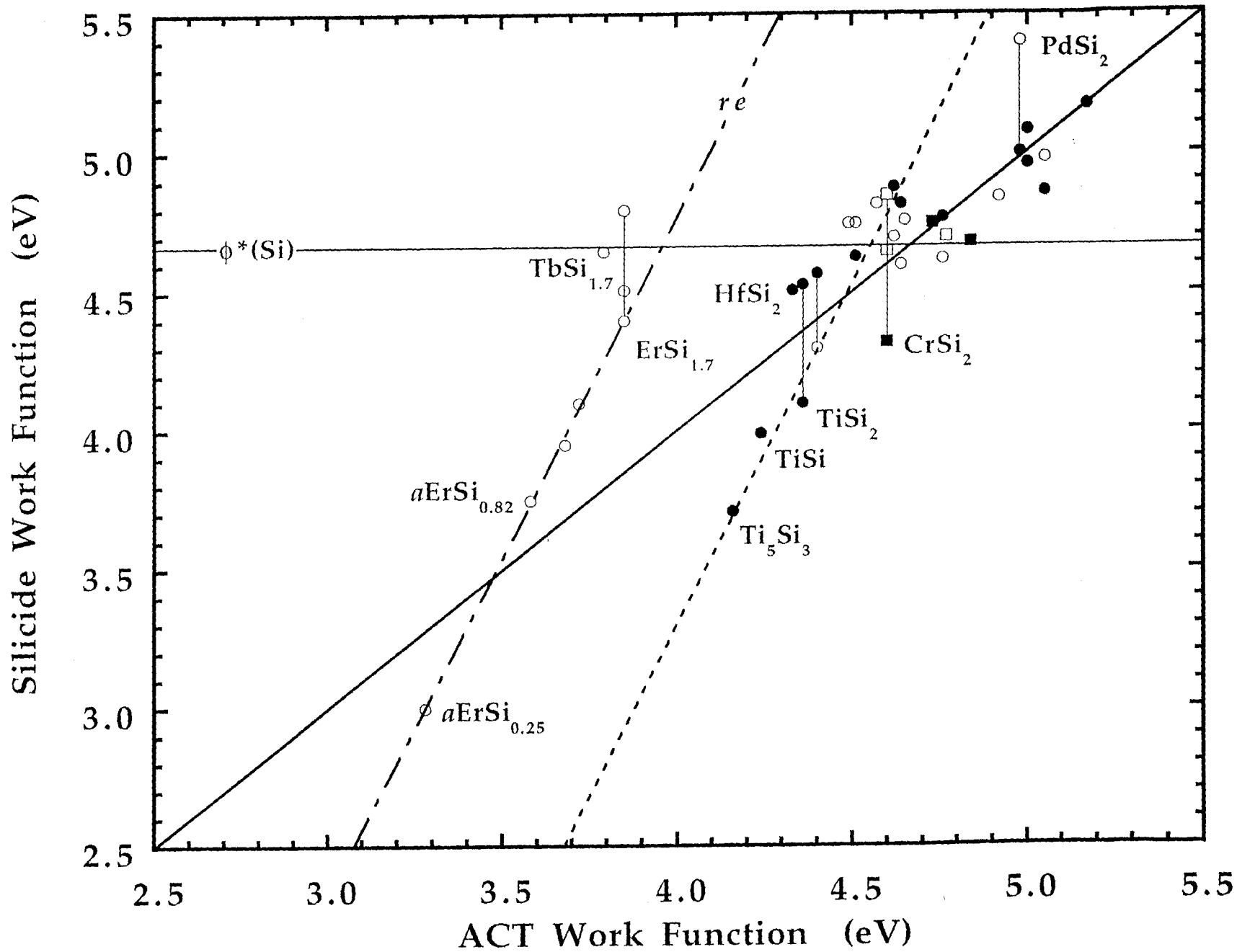


Figure 6